Angewandte Chemie
Eine Zeitschrift der Gesellschaft Deutscher Chemiker

# Supporting Information

69451 Weinheim, Germany

# Supplementing Information: Molecular Dynamics Simulation of Benzene Diffusion in MOF-5: Importance of Lattice Dynamics

Saeed Amirjalayer, Maxim Tafipolsky, and Rochus Schmid*

September 14, 2006

[*]
Lehrstuhl für Anorganische Chemie II
Organometallics and Materials Chemistry
Ruhr-Universität Bochum
44780 Bochum (Germany)

E-mail: rochus.schmid@rub.de

## 1 Computational Details and Forcefield

All MD simulations were performed with the *tinker* program package developed by J. Ponder. [1] The MM3 forcefield as implemented in the *tinker* code was used. All details of the parameterization procedure and validation of the complete forcefield are published separately. [2] The main issue was a parameterization for the $Zn_4O$ nodal unit of MOF-5, where the interactions between the Zn and O atoms were treated as partially covalent. In addition to that also the $C_{ph} - C_{carb}$ bond in the terephthalate moiety and some terms in the carboxylic acid group had to be reparameterized, with a special focus on the phenylene torsional barrier. All parameters were derived from DFT calculations of model fragments like $(Zn_4O)(O_2C-Ph)_6$ and $(C_6H_4)[(HCO_2)_5(Zn_4O)]_2$ and were tuned to reproduce both the geometry and the vibrational normal modes. Bond dipole parameters were generated from atomic charges fitted to the eletrostatic potential using the Merz-Kollman sampling scheme. [3] The final parameter set, which was used in this study is summarized in Tab. 1.

## 2 Molecular Dynamics Simulations

The MD simulations were performed with a timestep of 1.0 fs, which was checked to yield energy conserving microcanonic dynamics with the modified Beeman propagator as implemented in the *tinker* code. [4, 5] Both empty and benzene loaded constant pressure dynamics (NPT ensemble) showed negligible oscillations in the lattice parameters. Thus, an NVT ensemble was sampled for both rigid and flexible framework simulations with a lattice size 25.9457 Å. This value results from a lattice minimization of MOF-5. On a discussion of the different calculated and measured lattice parameters of MOF-5 we refer here to Ref. [2]. Each trajectory was started from a different configuration, generated from a high temperature simulation at 1000 K. The initial velocities were randomly generated according to a Boltzmann distribution at a given temperature, and the temperature was held constant by the Berendsen thermostat. [6] In case of the flexible model we verified the temperature to be held at the desired value also for the subsystem of the ten benzene molecules. The first 500 ps were discarded as an equilibration period. From the 3 ns trajectories the last 2.5 ns were used for the analysis, with a configuration stored every 0.1 ps (every 100 timesteps). Thus, per trajectory a total of 25,000 configurations were stored and used for the further analysis. The probability density was generated from the folded COM trajectories in a $20^3$ point mesh of the unit cell and was analyzed and rendered with the program *XCrysDen*. [7] We have refrained from symmetrizing the distribution in order to also visualize the remaining deficiencies in the sampling.

# 3 Results

## 3.1 Self-Diffusion Coefficients

From the 25,000 stored configurations of each trajectory, the MSD($\Delta t$) curves (see Fig. 1 of the manuscript) were calculated from the benzene COM using multiple time origins and time intervals from 0.1 ps up to 2500 ps, and by averaging over all values for a given time interval $\Delta t$ and all guest molecules. Thus, the jitter in the corresponding curves becomes larger for larger $\Delta t$, because of the decreasing quality in the statistics as less datapoints are available. For the further analysis we have closely followed the strategy described in Ref. [8]. The slope of the MSD($\Delta t$) curves have been determined from a linear fit to these curves in the range of time intervalls from $\Delta t = 250$ to 1000 ps. As proposed in Ref. [8] the lower value was chosen to be above the onset of the diffusive regime (see double logarithmic inset in Fig. 1 of the mansucript) and the larger value where the curves are still reasonably linear. Thus, the resulting slopes represent also an average over this range of time intervals. All corresponding self-diffusion coefficients $D_{self}$ for the individual trajectories are summarized in Tab. 2. The error estimates of the diffusion coefficients and the activation energies are twice the standard error calculated from the standard deviation from 15 trajectories.The final value and the corresponding error bars have been calculated from the average over the uncorrelated trajectories. Note that the error is just an approximation, since the error in the self-diffusion is harder to sample than the value itself.[8] Therefore we consider twice the standard error (standard deviation of the mean value) as a good measure for the statistical accuracy. In Tab. 3 the final values and errors of $D_{self}$ are summerized.

## 3.2 Binding energy

We have determined the “zero Kelvin” binding energy of a benzene molecule in the A cell pocket (with respect to MOF-5 and a single benzene molecule) for the rigid and flexible lattice with 41.39 kJ/mol and 41.48 kJ/mol, respectively. This global energy minimum was located by consecutive simulated annealing steps, and corresponds to a benzene molecule parallel to the face of the $Zn_4O$ tetrahedron, slightly displaced from the threefold symmetry axis. It appears to be very similar to the structure shown in Ref. [9], where unfortunetaly no calculated binding energy was given. The depth of the energy well is increased by only 0.09 kJ/mol for the flexible lattice, in contrast to the effect on the activation energy for the diffusion.

## 3.3 Benzene Center of Mass Probability Distribution

In Tab. 4 the probability density integrated for the individual A and B cells for the flexible and rigid framework are given in detail.

In Fig. 1 a contour plot of the difference of the COM probability distribution through the plane of the maxima of the pockets for the flexible and the rigid system is shown for a temperture of 300 K. Despite the slightly increased statistical noise, it is obvious that the population of the guest molecules in the binding pockets increases when the lattice dynamics is taken into account. The maximum of the probability distribution in the binding pocket is increased by roughly a factor of three. Correspondingly, the probability in the cell interiour (also in the B cells) is decreased. Thus, the benzene molecules are “attracted” by the framwork due to its ability to structurally adapt in case of the flexible model. Note that this mechanism is entirely different from the case of methane diffusion through carbon nanotubes, where the decrease of specular reflectance is the reason for a decrease of the diffusivity in the flexible model.[10]

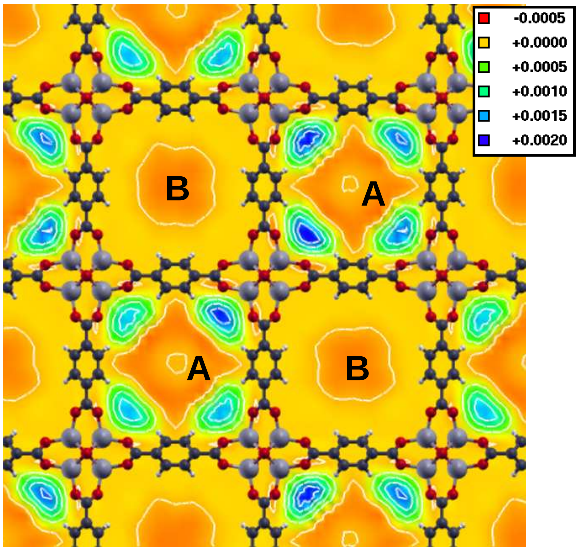

Figure 1: The difference in the probability density of the flexible and rigid model (at 300 K; slice through the maxima of the binding pockets). Positive values indicate an increased probability in the flexible model.

## References

[1] J. W. Ponder, F. M. Richards, *J. Comput. Chem.* **1987**, *8*, 1016., tinker version 4.2, June 2004; http://dasher.wustl.edu/tinker/.

[2] M. Tafipolsky, S. Amirjalayer, R. Schmid, *J. Comput. Chem.* Submitted.

[3] B. H. Besler, K. M. Merz, P. A. Kollman, *J. Comput. Chem.* **1990**, *11*, 431.

[4] D. Beeman, *J. Comput. Phys.* **1976**, *20*.

[5] B. R. Brooks, Algorithms for Molecular Dynamics at Constant Temperature and Pressure, *Internal report of division of computer research and technology*, National Institutes of Health, **1988**.

[6] H. J. C. Berendsen, J. P. M. Postma, W. F. van Gunsteren, A. DiNola, J. R. Haak, *J. Chem. Phys.* **1984**, *81*, 3684.

[7] A. Kokalj, *Comp. Mater. Sci.* **2003**, *28*, 155.

[8] R. Chitra, S. Yashonath, *J. Phys. Chem. B* **1997**, *101*, 5437.

[9] J. Gonzalez, R. N. Devi, D. P. Tunstall, P. A. Cox, P. A. Wright, *Micropor. Mesopor. Mater.* **2005**, *84*, 97.

[10] S. Jakobtorweihen, M. G. Verbeek, C. P. Lowe, F. J. Keil, B. Smit, *Phys. Rev. Lett.* **2005**, *95*(4), 044501.

Table 1: Additional force field parameters for MOF-5.

| | Bond stretches | |
|---|---|---|
| Atom types | Reference distance, Å | Force parameter, mdyn/Å |
| Zn-O$_{\text{cent}}$ | 2.075 | 0.85 |
| Zn-O$_{\text{carb}}$ | 2.015 | 0.85 |
| C$_{\text{carb}}$-O$_{\text{carb}}$ | 1.285 | 7.54 |
| C$_{\text{carb}}$-C$_{\text{ph}}$ | 1.480 | 4.84 |
| C$_{\text{ph}}$-C$_{\text{ph}}$ | 1.38 | 6.56 |
| | In-plane angle bending | |
| | Reference angle, deg | Force parameter, mdyn Å/rad$^2$ |
| Zn-O$_{\text{cent}}$-Zn | 109.471 | 0.40 |
| O$_{\text{cent}}$-Zn-O$_{\text{carb}}$ | 111.3 | 0.30 |
| O$_{\text{carb}}$-Zn-O$_{\text{carb}}$ | 107.6 | 0.22 |
| Zn-O$_{\text{carb}}$-C$_{\text{carb}}$ | 131.2 | 0.43 |
| O$_{\text{carb}}$-C$_{\text{carb}}$-O$_{\text{carb}}$ | 125.5 | 0.64 |
| C$_{\text{ph}}$-C$_{\text{ph}}$-C$_{\text{carb}}$ | 120. | 0.73 |
| O$_{\text{carb}}$-C$_{\text{carb}}$-C$_{\text{ph}}$ | 117. | 0.78 |
| | Out-of-plane angle bending | |
| (O$_{\text{carb}}$,O$_{\text{carb}}$)C$_{\text{carb}}$-C$_{\text{ph}}$ | 0.0 | 0.46 |
| | Stretch-bend (mdyn/rad) | |
| Zn-O$_{\text{cent}}$/Zn-O$_{\text{cent}}$-Zn | 0.4 | |
| | Torsional parameters (kcal/mol) | |
| | $V_0$ | |
| C$_{\text{ph}}$-C$_{\text{ph}}$-C$_{\text{carb}}$-O$_{\text{carb}}$ | 2.0 | |
| O$_{\text{cent}}$-Zn-O$_{\text{carb}}$-C$_{\text{carb}}$ | 10.0 | |
| Zn-O$_{\text{cent}}$-Zn-O$_{\text{carb}}$ | 10.0 | |
| Zn-O$_{\text{carb}}$-C$_{\text{carb}}$-O$_{\text{carb}}$ | 10.0 | |
| Zn-O$_{\text{carb}}$-C$_{\text{carb}}$-C$_{\text{ph}}$ | 10.0 | |
| | Bond dipoles (D) | |
| Zn-O$_{\text{cent}}$ | 3.352 | |
| Zn-O$_{\text{carb}}$ | 2.794 | |
| C$_{\text{carb}}$-O$_{\text{carb}}$ | 2.255 | |
| C$_{\text{carb}}$-C$_{\text{ph}}$ | -0.432 | |
| C$_{\text{ph}}$-H | -0.6 | |
| | Van der Waals parameters | |
| | radius, Å | $\varepsilon$, kcal/mol |
| Zn | 2.29 | 0.276 |
| O | 1.82 | 0.059 |
| C | 1.94 | 0.056 |
| H | 1.62 | 0.020 |

Table 2: $D_{self}$ in units of $10^{-9}\frac{m^2}{s}$ from the individual trajectories (linear fit of averaged MSD($\Delta t$) curve for the range of time intervals from 250 to 1000 ps; see text)

| | flexible | | | | rigid | | | |
|---|---|---|---|---|---|---|---|---|
| T [K] | 250 | 300 | 350 | 400 | 250 | 300 | 350 | 400 |
| 1 | 0.53 | 2.37 | 5.20 | 7.67 | 12.83 | 26.67 | 27.51 | 25.69 |
| 2 | 1.36 | 1.42 | 6.28 | 5.08 | 13.11 | 19.35 | 26.30 | 34.42 |
| 3 | 0.71 | 2.80 | 5.88 | 7.63 | 11.54 | 16.18 | 19.60 | 34.90 |
| 4 | 0.88 | 2.08 | 6.37 | 5.51 | 8.76 | 20.37 | 17.27 | 23.91 |
| 5 | 0.48 | 3.96 | 6.46 | 5.80 | 14.41 | 19.44 | 21.37 | 25.75 |
| 6 | 0.47 | 2.13 | 3.88 | 6.96 | 8.45 | 18.14 | 23.63 | 34.82 |
| 7 | 0.53 | 2.44 | 5.16 | 9.72 | 20.09 | 19.01 | 19.84 | 25.20 |
| 8 | 0.48 | 2.91 | 3.79 | 12.90 | 13.52 | 18.58 | 28.29 | 24.52 |
| 9 | 0.47 | 2.58 | 6.89 | 8.73 | 9.95 | 24.77 | 22.41 | 20.53 |
| 10 | 0.68 | 2.33 | 4.95 | 11.88 | 11.53 | 16.35 | 18.21 | 28.72 |
| 11 | 0.64 | 2.58 | 4.92 | 12.91 | 16.11 | 20.17 | 20.67 | 22.83 |
| 12 | 0.31 | 2.48 | 5.34 | 6.12 | 9.60 | 13.17 | 17.31 | 29.67 |
| 13 | 0.77 | 2.25 | 6.03 | 8.70 | 13.06 | 22.09 | 21.75 | 27.51 |
| 14 | 0.98 | 1.93 | 4.20 | 5.99 | 11.92 | 13.47 | 22.97 | 27.25 |
| 15 | 0.80 | 3.01 | 3.33 | 8.46 | 15.24 | 24.49 | 27.01 | 22.39 |

Table 3: Calculated self diffusion coefficients $D_{self}$ and the corresponding errors $\Delta D_{self}$ (twice the standard error) for a flexible and rigid lattice derived from values in Tab. 2.

| | flexible | | rigid | |
|---|---|---|---|---|
| T [K] | $D_{self}$ [$\frac{m^2}{s}$] | $\triangle D_{self}$ [$\frac{m^2}{s}$] | $D_{self}$ [$\frac{m^2}{s}$] | $\triangle D_{self}$ [$\frac{m^2}{s}$] |
| 250 | 0.67 x $10^{-9}$ | 0.14 x $10^{-9}$ | 12.7 x $10^{-9}$ | 1.6 x $10^{-9}$ |
| 300 | 2.49 x $10^{-9}$ | 0.29 x $10^{-9}$ | 19.5 x $10^{-9}$ | 2.0 x $10^{-9}$ |
| 350 | 5.25 x $10^{-9}$ | 0.56 x $10^{-9}$ | 22.3 x $10^{-9}$ | 1.9 x $10^{-9}$ |
| 400 | 8.27 x $10^{-9}$ | 1.34 x $10^{-9}$ | 27.2 x $10^{-9}$ | 2.3 x $10^{-9}$ |

Table 4: Benzene center of mass populations in the A and B cells at $T$ =300 K.

| | flexible framework | | | | |
|---|---|---|---|---|---|
| | 1 | 2 | 3 | 4 | sum |
| A | 0.222 | 0.250 | 0.218 | 0.233 | 0.924 |
| B | 0.019 | 0.018 | 0.018 | 0.020 | 0.076 |
| | rigid framework | | | | |
| | 1 | 2 | 3 | 4 | sum |
| A | 0.1829 | 0.1905 | 0.1896 | 0.1887 | 0.752 |
| B | 0.0628 | 0.0603 | 0.0618 | 0.0633 | 0.248 |